LOW LOSS DOPED STRONTIUM HEXAFERRITE SYNTHESIZED BY WOWS SOL-GEL METHOD

G. ASGHAR[a*], M. IRSHAD[b], N.A. NIAZ[c], S. NASIR[d], M.S. AWAN[e],
G.H.TARIQ[f], M. ANIS-UR-REHMAN[g]
[a]*Department of Physics, The University of Poonch Rawalakot AJK, Pakistan,*
[b]*Department of Chemistry, The University of Poonch Rawalakot AJK, Pakistan,*
[c]*Department of Physics, Bahauddin Zakariya University Multan, Pakistan,*
[d]*Department of Physics, University of Kotli AJK*
[e]*Department of* Nano-*Sciences* and Catalysis, *National Centre for Physics, Islamabad*
[f]*Department of Basic Sciences & Humanities, Khawaja Fareed University of Engineering and Information Technology Raheem Yaar Khan*
[g]*Applied Thermal Physics Laboratory, Department of Physics, COMSATS Institute of Information Technology, Islamabad 44000, Pakistan.*

M-type strontium hexaferrite with nominal composition $SrFe_{12-2x}Cr_xZn_xO_{19}$ with X = 0.0, 0.2, 0.4, 0.6, 0.8 is synthesized with WOWS (without water and surfactants) sol-gel method. Variation in lattice parameters, X-ray density and phase formation are studied by using the data obtained from X-ray diffraction patterns. The absence of any impurity peak confirms the formation of single phase of all doped samples. Frequency dependent ac electrical properties such as dielectric constant, dielectric loss and ac conductivity are studied by using precession component analyzer. Results indicates that the loss decreases with increase in doping content. Thus doping of Cr-Zn in strontium hexaferrite made this material useful for devices operating at high frequency.

1. Introduction

M-type hexaferrites are being widely used in industry and in domestic appliances. M-type hexaferrites can also be used in bulk form in many electronic devices, electrical devices, small motors, microwave devices and magnetic recording media {1-3] due to their excellent electrical and magnetic properties. M-type hexaferrites are famous for their high coercivity [4], large uniaxial magnetocrystalline anisotropy, high saturation magnetization, high Curie temperature good chemical stability and high corrosion resistivity. In order to fulfil the requirements of many applications such as recording media, microwave devices, permanent magnets and magneto-optics [5-6], etc. researchers are continuously working to tailor the properties of hexaferrites. The magnetic and dielectric properties of strontium hexaferrite can be tailored by replacing ferric ion (Fe^{3+}) with the ion of other element having same or different valency. If Fe^{3+} ion with spin down is replaced by such an ion whose unpaired electrons are less than that of Fe^{3+} ion then the number of unpaired electrons with the spin up would be increases. As a result net magnetic moment will increase because the net magnetic moment of one formula unit of strontium hexaferrite arises because of the difference of the spin up and spin down electrons. This increase in net magnetic moment will result in the increase in saturation magnetization. Similarly if Fe^{3+} ion with spin up is replaced by such an ion whose unpaired electrons are less than that of Fe^{3+} ion then the number of unpaired electrons with the spin up would be decreased. As a result net magnetic moment will decrease and hence saturation magnetization will decrease. The coercivity mainly depends upon

---

* Corresponding author: g.as70@yahoo.com

magneto crystalline anisotropy and microstructural parameters such as grain size, stresses in the crystal lattice, porosity, vacancies, spin canting and impurities. The high magneto crystalline anisotropy results in high coercivity. Strontium hexaferrite (M-type hexaferrite) is considered as hard magnet due to their high magneto crystalline anisotropy. The decrease in grain size (single domain) and increase in porosity and impurities increases the coercivity of the material and vice versa. The intrinsic coercivity of strontium hexaferrite is also very high (about 7 kOe). The coercivity of this material has been has been increased as high as ~13kOe and decreased to few hundred oestered according to its requirement for different applications [7].

The main source of dielectric loss in ferrites is conduction of electrons. In ferrites, the conduction is because of the electron hopping from Fe^{2+} and Fe^{3+} ion present on octahedral B sites [8-9]. The presence of this Fe^{2+} also contributes a lot to the dielectric properties of ferrites. It is reported in the literature that Cr^{3+} ions preferentially occupy octahedral B sites [10] where it replaces Fe^{3+} ions. It impedes the motion of charge carriers and results in the increase in coercivity and resistance. It is also reported that when Zn^{2+} being a divalent ion is doped in M-type hexaferrites, it preferentially occupy tetrahedral (A) site where it replaces Fe^{3+} ions. For the charge neutrality, Fe^{2+} ions present on octahedral (B) are changed to Fe^{3+} ions and hence the concentration of Fe^{2+} ions decreases. Keeping this thing in view, Cr^{3+} and Zn^{2+} were doped to decrease the concentration of Fe^{2+} ions in the structure and hence to decrease the dielectric losses and to increase coercivity.

Cr-Zn doped strontium hexaferrite with composition $SrFe_{12-2x}Cr_xZn_xO_{19}$ with $(X = 0.0, 0.2, 0.4, 0.6, 0.8)$ is synthesized by simplified sol-gel method. This new method is developed in our lab and is named as WOWS (With Out Water and Surfactants) sol-gel method [11].

2. Experimental

M-type strontium hexaferrite was prepared by WOWS sol-gel method. This method has number of advantages over other sol-gel methods. This method does not require surfactants or templates [11]. In WOWS sol-gel method, stoichiometric amounts of different precursors are dissolved in ethylene glycol. The molar ratio between metal salts to ethylene glycol is kept at 1:14 to dissolve the metal salts homogeneously.

The proposed reaction for all the nitrates with ethylene glycol is
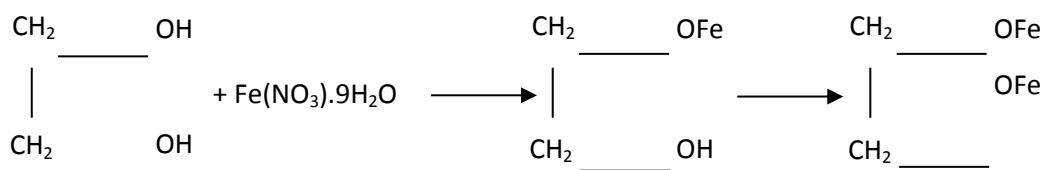
The salts used for the preparation of M-type strontium hexaferrite with nominal composition $SrFe_{12-2x}Cr_xZn_xO_{19}$ with X = 0.0, 0.2, 0.4, 0.6, 0.8 were $Sr(NO_3)_2$, $Fe(NO_3)_3 \cdot 9H_2O$, $Cr(NO_3)_3 \cdot 9H_2O$, $Zn(NO_3)_2 \cdot 6H_2O$. The pH of solution was 1. The solution is stirred for 30 min at room temperature in order to prepare homogeneous solution. The temperature of this solution is raised to 100^oC with continuous stirring. By doing so, a thick gel is formed. The gel so obtained is heated to 300^oC. At 300^oC, the gel dried and burned slowly and transformed into fine powder. The dried powder is annealed in a box furnace for 1 h at 940 ±5 ∘C. This annealed powder is converted into pellets by using a uni-axial press. These pellets are sintered at 910 ±5 ∘C for 15 min and are used for different characterizations.

3. Results and discussion

3.1. Structural studies

The phase formation studies of the composition $SrFe_{12-2x}Cr_xZn_xO_{19}$ with (X = 0.0, 0.2, 0.4, 0.6, 0.8), prepared by WOWS sol-gel method, are made by using powder X-ray diffraction data. All the peaks of X-ray diffraction (XRD) patterns shown in figure 1 are identified by using ICDD patterns with reference code 01-080-1197. The indexed XRD patterns show that all the compositions have single phase of strontium hexaferrite material. This confirmed the successful substitution of Cr and Zn cations on the interstitial sites of strontium hexaferrite lattice as there is no separate peak of these substituted cations detected. The parameters calculated from XRD patterns are given in table 1. Both lattice parameters a & c are increased with the increase in Cr-Zn concentration. This change is attributed to Zn^{2+} whose ionic radius is greater than that of Fe^{3+} ion [12]. The replacement of large cation on the interstitial sites of strontium hexaferrite causes the crystal structure to expand and in other words lattice parameters increases and X-ray density decreases.

The lattice parameters (a & c) of hexagonal crystal structure can be calculated by using the formula

$$\frac{1}{d^2} = \frac{4}{3}\left(\frac{h^2+hk+k^2}{a^2}\right) + \frac{l^2}{c^2} \qquad \text{1)}$$

where 'hkl' are Miller indices and 'd' is the interplaner spacing.

The crystallite size 'D' is calculated by using Full Width at Half Maximum (FWHM), obtained from the diffraction peaks in Scherrer's formula given by

$$D = \frac{0.89\lambda}{\beta Cos\theta} \qquad (2)$$

where 'λ' is wave length, 'β' is FWHM and 'θ' is the Bragg angle
X-ray density (theoretical density) is calculated by the formula

$$\rho_x = \frac{nM_m}{VN_A} \qquad (3)$$

where 'n' is number of formula units per unit cell, 'M_m' is the molar mass, 'V' is the volume of unit cell and 'N_A' is the Avogadro's number.
Bulk density is calculated by the formula

$$\rho_m = m/v \qquad (4)$$

where m is mass and v is the volume
Porosity is calculated by the formula

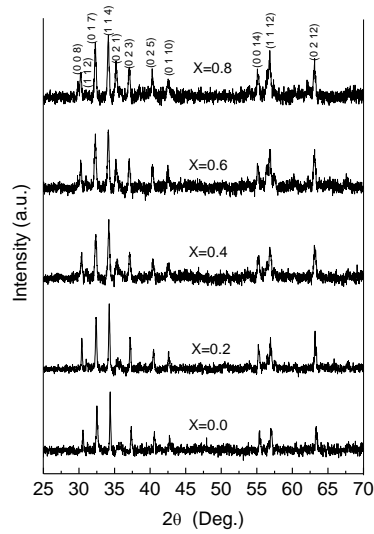$$P = 1 - \frac{\rho_m}{\rho_x} \qquad (5)$$

*Fig 1. Indexed XRD patterns of SrFe$_{12-2x}$Cr$_x$Zn$_x$O$_{19}$ (X=0.0, 0.2, 0.4, 0.6, 0.8)
prepared by WOWS sol-gel method.*

2.2 Dielectric properties

For solids, Maxwell-Wagner two layer model is being commonly used to discuss their dielectric properties. According to Maxwell-Wagner two layer model, the grain in a bulk material acts as a resistor and grain boundary acts as thin insulating layer discussed earlier. The dielectric properties are measured at room temperature in the frequency range (10kHz-3MHz) using precision component analyzer.

In ferrites, as described earlier, the polarization mechanism is similar to their conduction mechanism i.e. because of the electron hopping from Fe^{2+} and Fe^{3+} ion present on octahedral B sites. The presence of this Fe^{2+} also contributes a lot to the dielectric properties of ferrites. It is reported in the literature that Cr^{3+} ions preferentially occupy octahedral B sites [13] where it replaces Fe^{3+} ions and increases the concentration of Fe^{2+} ions by transforming Fe^{3+}-Fe^{2+} for higher Cr content. Zn^{2+} ions preferentially occupy tetrahedral A and may also occupy bipyramidal C sites [14] where it replaces Fe^{3+}. For charge neutrality, the Fe^{2+} ions present on octahedral B site [15-16] are converted into Fe^{3+} ions.

Table 1: Lattice parameters (a & c), crystallite size (D$_{114}$), X-ray density (ρ$_x$), bulk density (ρ$_m$), % porosity, dielectric constant (ε'), dielectric loss tangent (tanδ) and ac conductivity (σ$_{ac}$) of the prepared samples of SrFe$_{12-2x}$Cr$_x$Zn$_x$O$_{19}$ ($X = 0.0, 0.2, 0.4, 0.6, 0.8$) by WOWS sol-gel method.

SrFe$_{12-2x}$Cr$_x$Zn$_x$O$_{19}$	X=0.0	X=0.2	X=0.4	X=0.6	X=0.8
Lattice Constant					
a(Å)	5.868(2)	5.879(3)	5.886(2)	5.892(2)	5.891(2)
c(Å)	23.008(1)	23.009(2)	23.014(4)	23.032(3)	23.059(6)
c/a	3.92	3.91	3.91	3.91	3.91
X-ray Density ρ$_x$ (g/cm^3)	5.14	5.12	5.11	5.10	5.09
Bulk Density ρ$_m$ (g/cm^3)	2.82(2)	2.13(1)	2.16(2)	2.28(2)	2.32(3)
% Porosity	45	58	58	55	54
Dielectric constant (ε') at 3MHz	5.53(1)	5.35(1)	4.92(1)	4.72(1)	4.58(1)
Dielectric loss (tanδ) at 3MHz	0.037(1)	0.038(1)	0.035(1)	0.028(1)	0.023(1)

2.2.1. The dielectric constant (ε')

The values of capacitance (C) obtained from precision component analyzer at different frequencies are used to calculate dielectric constant (ε') using the formula:

$$\varepsilon' = \frac{Cd}{A\varepsilon_0} \tag{6}$$

where 'd', 'A' and 'ε_0' are the thickness, area of pellet and is the permittivity of free space respectively.

The graph shown in figure 2 reveals that the dielectric constant ε' for all compositions decreases sharply at lower frequencies and then becomes fairly constant for higher frequencies. The dielectric polarization mechanism in ferrites is similar to their conduction mechanism. At low frequency, the electron could easily follow the applied field and the time available for electrons to hope from one site to other sites is more. Hence more the displacement of charge could take place inside the grain and hence causes large dielectric constant. At high frequency, the hoping of the charge could not follow the applied field and only local charge polarization could take place and hence net dielectric constant decreases. The graph also indicates that ε' has a decreasing trend with the increase in doping contents. This is due to the fact that in ferrites, the space charge polarization directly depends upon Fe^{2+} ion concentration in a grain.
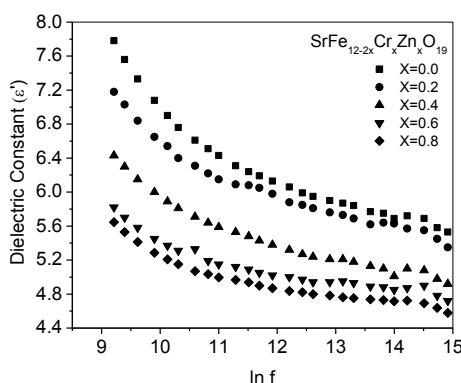

Fig. 2: Plot of dielectric constant (ε') as a function of ln of frequency for
$SrFe_{12-2x}Cr_xZn_xO_{19}$ (X=0.0, 0.2, 0.4, 0.6, 0.8) prepared with WOWS sol-gel method

As Zn^{2+} ions have strong preference to occupy tetrahedral (A) sites, so concentration of Fe^{2+} ions on tetrahedral site decreases as explained earlier. So electric polarization decreases and consequently ε' decreases. This may also be due to the reason that the Cr ions do not participate in the conduction process but impedes the transformation of Fe^{2+} - Fe^{3+} ions [17-18].

2.2.2 The dielectric loss tangent ($tan\delta$)

Dissipation factor (D) obtained from precision component analyzer at different frequencies is taken as dielectric loss tangent ($tan\delta$). The general trend of the dielectric loss tangent ($tan\delta$) shown in figure 3 could be explained in terms of conduction losses which are the main source of dielectric losses. A relation between conduction and dielectric losses was discussed by Iwauchi et al. [19].
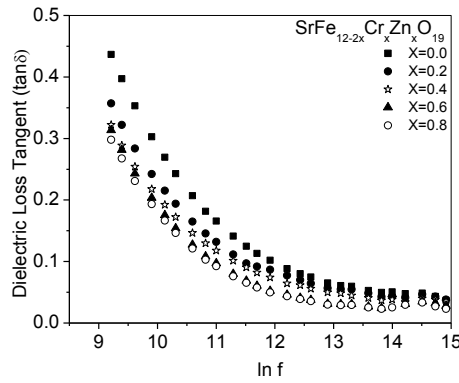
Fig 3: Plot of dielectric loss tangent (tanδ) as a function of ln of frequency for SrFe$_{12-2x}$Cr$_x$Zn$_x$O$_{19}$ (X=0.0, 0.2, 0.4, 0.6, 0.8) prepared with WOWS sol-gel method

According to Iwauchi, charge polarization in ferrites is similar to their electrical conduction mechanism. In lower frequency region, the dielectric loss tangent is more than at high frequency region. It is due to the fact that lower the frequency, more the time available for the displacement of the charge inside the grains which acts as a conductive medium, more would be the conduction and higher would be the dielectric losses. As the frequency increases, the electron hopping could not follow the applied frequency, the conduction inside the grain decreases and hence dielectric loss tangent decreases. Figure 3 shows that the dielectric loss tangent also decreases with the increase in doping concentration. This may be due to the decrease in Fe^{2+} ion concentration, which is responsible for conduction losses, because of increase in Zn^{2+} content as explained earlier. This may also be due to the increase in lattice parameters. The values of dielectric loss tangent obtained from this composition of strontium hexaferrite are much smaller than reported in [20-21]. So it is expected that this substitution (X=0.2 to 0.8) would also be more suitable for the devices operating at high frequencies than already reported composition.

2.2.3 The ac conductivity (σ_{ac})

The ac conductivity (σ_{ac}) is calculated by using the equation 7. Fig. 4 show that σ_{ac} is fairly constant for a range of low frequencies and then starts increasing at higher frequencies. The

$$\sigma_{ac} = \varepsilon_0 \varepsilon' \tan\delta \tag{7}$$

hoping frequency of electron is small at lower frequencies and it increases with the increase in frequency. This is attributed to the fact that the required energy correlated with forward-backward hoping is only a fraction of the energy necessary to activate long range diffusive conduction [22]. The decrease in σ_{ac} with the increase in Cr-Zn concentration is due to decrease in Fe^{2+} ion concentration discussed earlier.
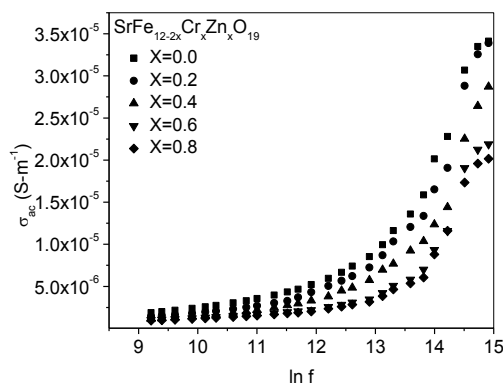
Fig 4: Plot of ac conductivity (σ_{ac}) as a function of ln of frequency for SrFe$_{12-2x}$Cr$_x$Zn$_x$O$_{19}$ (X=0.0, 0.2, 0.4, 0.6, 0.8) prepared with sol-gel method
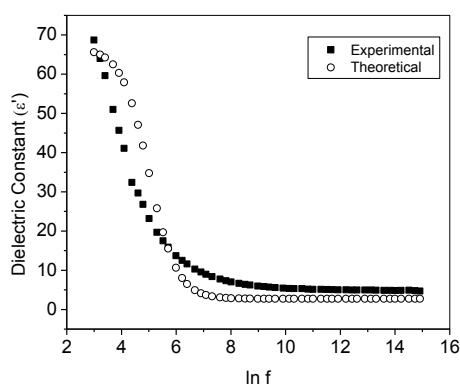

Fig 5: Plot of experimental and theoretically calculated dielectric constant (ε') for the sample X=0.6 (SrFe$_{12-2x}$Cr$_x$Zn$_x$O$_{19}$) as a function of frequency

Fig. 5 shows the plot of theoretically calculated values by using the equation 8 and

$$\varepsilon' = \varepsilon_\infty + \frac{\varepsilon_s - \varepsilon_\infty}{1 + \omega^2 \tau^2} \tag{8}$$

experimentally observed measurements of dielectric constant of sample X=0.6 prepared by sol-gel method. The obtained results match well with the theoretical results. A small difference in both curves may be due to the fact that grain boundaries do not act as perfectly insulating regions. A leakage current takes place at grain boundaries. The leakage current is more at lower frequencies and less at higher frequencies.

3. Conclusions

The indexed XRD patterns of the composition SrFe$_{12-2x}$Cr$_x$Zn$_x$O$_{19}$ with X=0.0, 0.2, 0.4, 0.6, 0.8 prepared with WOWS sol-gel method indicate single phase formation as there is no impurity peak present in any of sample. This shows that WOWS sol-gel method provide much better control on cations distribution. The dielectric loss is small and shows a decreasing trend with doping concentration. The ac conductivity also decreases with the increase in Cr-Zn concentration. So Cr-Zn doping in strontium hexaferrite prepared with this method is useful for high frequency applications.

804

References

[1] V. P. Singh, G. Kumar, J. Shah, A. Kumar, M. Dhiman, R. K. Kotnala, M. Singh, Ceramics International **41,** 11693 (2015).

[2] H. Yamamoto, M. Nagakura, H. Terada, IEEE Trans. Magn. **26**, 1144 (1990).

[3] G. Li, G.G. Hu, H.D. Zhou, X.J. Fan, and X.G. Li, Mater. Chem. Phys. **75**, 101 (2002).

[4] F. Kools, A. Morel, R. Grossinger, J.M. Le Breton, and P. Tenaud, J. Magn. Magn. Mater. **1270**, 242 (2002).

[5] S. S. S. Afghahi, M. Jafarian, M. Salehi, Y. Atassi, J. Magn. Magn. Mater. **421,** 340 (2016).

[6] H. Pfeiffer, R.W. Chantrell, P. Gornert, W. Schuppel, E. Sinn, and M. Rosler, J. Magn. Magn. Mater. **125**, 373 (1993).

[7] Osamu Kohmoto, Takeo Tsukada, Shigeo Sato, Jpn. J. Appl. Phys., **29,** 1944 (1990).

[8] D. Seifert, J. Topfer, F. Langenhorst, J. M. L.. Breton, H. Chiron, L. Lechevallier, J. Magn. Magn. Mater. **321,** 4045 (2009).

[9] C. M. Fang, F. Kools, R. Metselaar, G. de With, R. A. de Groot, J. Phys: Condens. Mat., **15,** 6229 (2003).

[10] S. Ounnunkad, P. Winotai, J. Magn. Magn. Mater. **301,** 292 (2006).

[11] S. Nasir, M. Anis-ur-Rehman, M. A. Malik, Phys. Scr. 83 (2010).

[12] S. Nasir, G. Asghar, M. A. Malik, M. Anis-ur-Rehman, J Sol-Gel Sci Technol, (2011).

[13] S. Ounnunkad, P. Winotai, J. Magn. Magn. Mater. **301,** 292 (2006).

[14] A. G. Angeles, G. M. Suarez, A. Gruskova, M. Papanova, J. Slama, Mat. Letter. **59,** 26 (2005).

[15] M. J. Iqbal, M. N. Ashiq, I. H. Gul, J. Magn. Magn. Mater. **322**, 1720 (2010).

[16] M. Pal, P. Brahma, B. R. Chakraborty, D. Chakravorty, Jpn. J. Appl. Phys., **36,** 2163 (1997).

[17] A. A. Sattar, A. H. Wafik, H. M. El-Sayed, J. Mater. Sci., **36,** 4703 (2001).

[18] K. H. Rao, S. B. Raju, K. Aggarwal, R. G. Mendiratta, J. Appl. Phys. **52,** 1376 (1981).

[19] K. Iwauchi, Jpn. J. Appl. Phys. **10,** 1520 (1971).

[20] M. N. Ashiq, M. J. Iqbal, I. H. Gul, J. Alloys Compd., **487,** 341 (2009).

[21] M. J. Iqbal, M. N. Ashiq, P. H. Gomez, J. M. Munoz, J. Magn. Magn. Mater. **320,** 881 (2008).

[22] M. P. Kumar, T. Sankarappa, B. V. Kumar, N. Nagaraja, Solid State Sciences, **11,** 214 (2009),